sciendo

LATVIAN JOURNAL OF PHYSICS
AND TECHNICAL SCIENCES
2021, N 6

DOI: 10.2478/lpts-2021-0042

INFLUENCE OF "PRODUCTIVE" IMPURITIES (Cd, Na, O) ON THE PROPERTIES OF THE Cu_2ZnSnS_4 ABSORBER OF MODEL SOLAR CELLS

D. Sergeyev[1, 2*], N. Zhanturina[1*], A. Aizharikov[2], A.I. Popov[3*]

[1] K. Zhubanov Aktobe Regional University, Aktobe, KAZAKHSTAN
[2] T. Begeldinov Aktobe Aviation Institute, Aktobe, KAZAKHSTAN
[3] Institute of Solid State Physics, University of Latvia,
8 Kengaraga Str., Riga, LATVIA
*e-mail: serdau@mail.ru, nzhanturina@mail.ru, popov@latnet.lv

The study focuses on the optical properties of the CZTS multicomponent semiconductor absorber with 3 % "production" impurities of Cd, Na, O within the framework of the density functional theory using the generalized gradient approximation and the SCAPS program, as well as investigates their influence on the performance and efficiency of CZTS-solar cells. The results showed that the introduction of Cd, Na, O impurities would lead to a decrease in the intensity of the absorption bands at 2.06 eV and 2.55 eV. The density of states CZTS: (Cd, Na, O) was determined from first principles, and it was revealed that impurities of Cd and O atoms would lead to a decrease in the band gap (to 0.9 eV and 0.79 eV), and an increase in Na impurity absorption (1.2 eV). It was also found that a decrease in the band gap led to a decrease in the open circuit voltage, and it was also shown that "industrial" impurities led to a decrease in the efficiency of energy conversion of solar cells to 2.34 %.

Keywords: *Cu_2ZnSnS_4 (CZTS), density of states, JV-characteristics, optical absorption coefficient, SCAPS, solar cell.*

1. INTRODUCTION

Currently, one of the most emerging problems is the lack of energy resources and environmental pollution. For a comprehensive solution of these environmental tasks, it is of interest to use renewable energy sources, as well as to increase their share of consumption. Promising areas of alternative energy are the use of solar energy, the movement of air masses, ebb and flow, sea currents and others. To convert the listed types of energy into electrical energy, energy converters are needed, as well as efficient operation of power supply, energy storage devices are required. The solution to these problems will make it possible to create highly efficient, economical and environmentally-friendly power supply systems.

Note that various options have already been proposed and successfully developed for energy converters, such as solar batteries [1]–[3], wind generators [4], [5], geothermal converters [6], as well as for different energy storage devices, such as a superconducting inductive storage [7]. To improve the performance of these systems, new properties of solar radiation absorbers [8]–[10], quasi-two-dimensional materials [11]–[13], superconductors [14]–[16] and others are being searched.

Solar energy is the most economical and efficient among all the listed renewable energy sources. Therefore, in recent years, active work has been carried out to introduce alternative sources of power supply to various objects of special equipment with autonomous electricity based on photovoltaic modules using solar energy. To improve the output energy characteristics of such modules, the electronic properties of nanomaterials [17]–[20], due to quantum-size effects, are being intensively studied. The application of the quantum properties of quasiparticles can lead to a significant improvement in the basic parameters of photoelectronic devices.

It is impossible to develop new types of solar cells without understanding the ongoing physical and chemical processes when converting solar energy into electrical energy. Currently, work is underway to study thin-film solar cells based on Cu (In, Ga) (S, Se)2 (CIGS) [21]–[23]. This is due to the fact that they have high absorption coefficients and are relatively cheap [24]. However, despite the above advantages, thin-film solar cells based on CIGS are inferior to their counterparts in terms of efficiency and radiation resistance, and the elements In and Ga included in CIGS are highly toxic substances. In order to avoid the expensive disposal of such toxic elements for the creation of thin-film solar cells, the photovoltaic properties of environmentally-friendly materials are being intensively studied. By replacing highly toxic elements In, Ga, respectively, with non-toxic elements Zn, Sn, a multicomponent semiconductor compound Cu2ZnSn (S, Se)4 (CZTS) was obtained [25]. The unit cell of the CZTS structure is shown in Fig. 1.

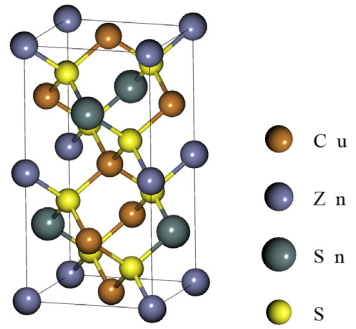

Fig. 1. Unit cell structure of CZTS.

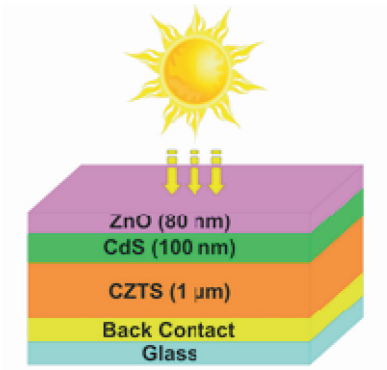

Fig. 2. Multicomponent solar cell model based on CZTS.

Thin-film solar cells based on $Cu_2ZnSn(S,Se)_4$ are a layered structure of the type ZnO/CdS/CZTS, i-ZnO/ZnS/CZTS, etc., see, for example, Fig. 2. Such layered and multicomponent structures are very complex and during production the absorber of the CZTS solar cell is contaminated with various impurities, for example, cadmium from the adjacent layer of CdS, Na from glass, as well as oxygen, nitrogen and hydrogen atoms penetrating from the air; therefore, we will call such impurities "production". Despite the low concentration of industrial impurities, they affect the optical characteristics of the absorber, which is important to take into account when developing high-performance solar cells.

In this paper, within the framework of the density functional theory using the generalized gradient approximation (DFT-GGA), the optical properties of the CZTS absorber with 3% Cd, Na and O impurities are determined, and the effects of these impurities are estimated using the SCAPS program (a Solar Cell Capacitance Simulator) on the electrical transport properties of a solar cell by the example of the structure i-ZnO/CdS/CZTS/glass.

2. SIMULATION MODEL AND METHODS

The procedure for optimizing the CZTS geometry and describing the interatomic interaction was carried out within the framework of the density functional theory (DFT); the generalized gradient approximation GGA-PBE was used as the exchange-correlation functional [26]. When optimizing the structures, the atomic configuration parameters were relaxed until the forces on all atoms became less than a predetermined threshold value of 0.05 eV/Å.

Computer simulation of the optical characteristics of CZTS, CZTS: Cd, CZTS: Na, CZTS: O was carried out within the DFT-GGA using the Kubo-Greenwood equation, which determined their dielectric susceptibility:

$$\chi_{ij}(\omega) = -\frac{e^2\hbar^4}{m_e^2\varepsilon_0 V\omega^2}\sum_{nm}\frac{f(E_m)-f(E_n)}{E_{nm}-\hbar\omega-i\hbar\Gamma}\pi^i_{nm}\pi^j_{mn}, \quad (1)$$

where π^i_{nm} is i-component of the dipole matrix element between state n and m; V – the volume; Γ – the broadening; e – the charge of the electron; $\hbar$ – Planck's constant; E – energy; $f(E)$ – the Fermi distribution function of quasiparticle energy; ε_0 – dielectric constant of vacuum; ω – frequency; m_e – electron mass.

From Eq. (1), the dependence of the dielectric constant on frequency (on energy) is determined:

$$\varepsilon(\omega) = 1 + \chi(\omega). \quad (2)$$

Using the imaginary and real parts of the dielectric constant (2), we find the extinction coefficient:

$$k(\omega) = \sqrt{\frac{\sqrt{\mathrm{Re}(\varepsilon)^2 + \mathrm{Im}(\varepsilon)^2} - \mathrm{Re}(\varepsilon)}{2}}. \quad (3)$$

From (3) optical absorption coefficient is determined:

$$\alpha = 2\frac{\omega}{c}k. \quad (4)$$

Simulation of optical properties of CZTS is done using program Atomistix ToolKit with Virtual NanoLab [27].

To determine the density of state of CZTS, we first calculate its local density of states (LDOS):

$$D(\varepsilon, r) = \sum_{ij} \rho_{ij}(\varepsilon)\phi_i(r)\phi_j(r), \quad (5)$$

where $\rho(\varepsilon) = \rho^L(\varepsilon) + \rho^R(\varepsilon)$, $\phi(r)$ – base orbitals. The density of states CZTS is obtained by integrating the LDOS over the entire space:

$$D(\varepsilon) = \int drD(\varepsilon) = \sum_{ij} \rho_{ij}(\varepsilon)S_{ij}, \quad (6)$$

where $S_{ij} = \int \phi_i(r)\phi_j(r)dr$ – the overlap matrix.

In this paper, the assessment of the influence of Cd, Na, O impurities on the output parameters of solar cells based on the CZTS absorber was carried out using the SCAPS program developed by the Department of Electronics and Information Systems (ELIS) of the University of Ghent [28]–[31]. Using the SCAPS program, the output energy parameters of multicomponent solar cells CZTS / CdS / i-ZnO / glass, CZTS: Cd / CdS / i-ZnO / glass, CZTS: Na / CdS / i-ZnO / glass, CZTS: O / CdS / i-ZnO / glass were simulated.

The calculation of the photovoltaic parameters of solar cells based on CZTS was carried out by numerically solving the basic equations of the semiconductor (Poisson's equation, which relates the electrostatic potential to the total charge density):

$$\frac{\partial}{\partial x} = \left(\varepsilon_0\varepsilon_r \frac{\partial\psi}{\partial x}\right) = -e\left(p - n - N_D^+ - N_A^- + \frac{\rho_{def}}{e}\right), \quad (7)$$

where ψ – electrostatic potential; ε_r – semiconductor dielectric constant; N_D^+ – ionized donor concentration; N_A^- – ionized acceptor concentration; p – free hole concentration; n – free electron concentration; ρ_{def} – defect charge density.

Drift and diffusion mechanisms of charge carrier transport in semiconductors are described, respectively, by the following equations:

$$J_n = D_n\frac{dn}{dx} + \mu_n n\frac{d\phi}{dx}, \quad (8.1)$$

$$J_p = D_p\frac{dp}{dx} + \mu_p p\frac{d\phi}{dx}, \quad (8.2)$$

where J_n and J_p – current density of electrons and holes; D_n and D_p – diffusion coefficients of electrons and holes; ϕ – electric field; μ_n and μ_p – mobility of electrons and holes, respectively.

The external quantum efficiency of a model solar cell is determined by the formula:

$$EQE = \frac{J_{ph}(\lambda)}{eF(\lambda)}, \quad (9)$$

where $J_{ph}(\lambda)$ – total photogenerated current density; $F(\lambda)$ – solar stream. Solar radiation AM 1.5 with a power density of 100 mW/cm^2 is used as a source of sunlight. Note that the SCAPS software calculates the photovoltaic parameters taking into account the Shockley-Reed-Hall recombination statistics.

The basic SCAPS equations are described in detail in [28]–[31].

3. RESULTS AND DISCUSSION

Figure 3 shows the results of calculating the optical characteristics of CZTS, CZTS: Cd, CZTS: Na, CZTS: O. As can be seen, a significant contribution to the extinction coefficient is made by the imaginary part of the dielectric constant (see Eq. (3)). CZTS absorbs radiation in a wide energy range of ~ 1.6–3 eV, forming 2 absorption bands at energies of 2.06 eV and 2.55 eV. Note that one more absorption band outside the considered interval appears at 1.2 eV.

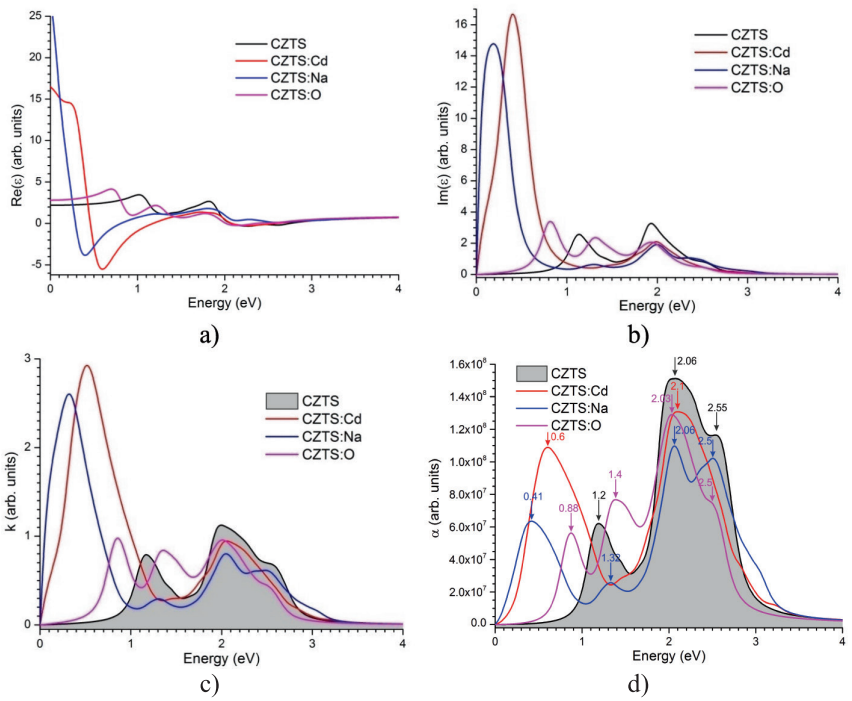

Fig. 3. Optical characteristics of the absorber CZTS:
a) real parts of the dielectric constant Re(ε);
b) complex parts of the dielectric constant Im(ε);
c) k is the extinction coefficient;
d) α – the optical absorption coefficient.

The introduction of 3 % Cd impurities, which replace mainly Zn atoms in the CZTS crystal lattice, will lead to a decrease in the intensity of the absorption spectrum at 2.1 eV; however, at 0.6 eV, a new band appears, and the band at ~ 1.2 eV disappears. An impurity of Na will also lead to a decrease in the intensities of the absorption band at 2.06 eV and 2.5 eV. The absorption band at 1.2 eV shifts to the high-energy side of 1.32 eV, and a new band appears at 0.41 eV. An impurity of an oxygen atom substituting a sulfur atom in the crystal lattice will lead, as in the case of other impurities, to a decrease in the intensity of the main absorption bands and their insignificant energy displacement of 2.03 eV and 2.5 eV. Moreover, in the low-energy region (at 0.88 eV and 1.4 eV), new absorption bands appear.

Figure 4 shows the results of calculating the density of states (DOS) CZTS, CZTS: Cd, CZTS:Na, CZTS:O. As can be seen, 3 % impurity of Cd and O atoms will lead to a decrease in the band gap from 1.1 eV to 0.9 eV and 0.79 eV, respectively, and the same concentration of Na impurity increases the band gap to 1.2 eV. Small changes in the CZTS bandgap affect other energy parameters of solar cells based on them.

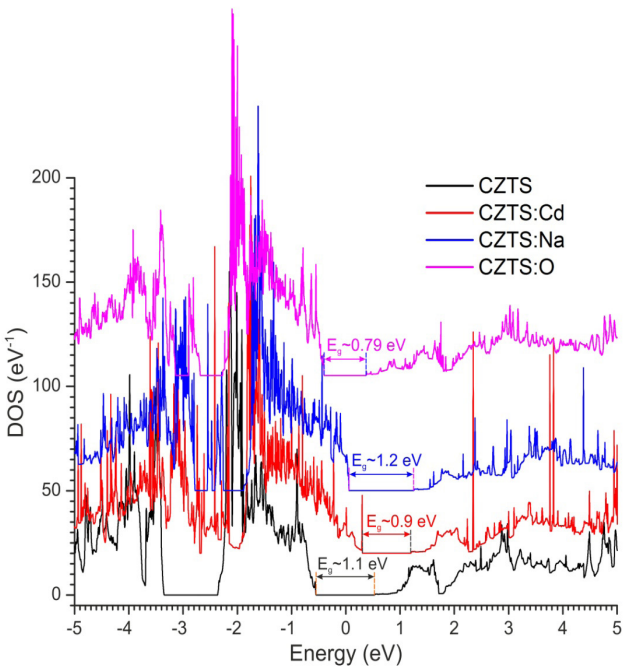

Fig. 4. Density of states of CZTS crystals.

Table 1 shows the main energy output parameters of a CZTS-based solar cell: (Cd, Na, O): open-circuit voltage (V_{oc}), short circuit current density (J_{sc}), fill factor (FF) and power conversion efficiency (PCE). As can be seen, with a decrease in the band gap in CZTS: Cd, CZTS: O, the open circuit voltage V_{oc} noticeably decreases from ~ 0.3 V to 0.19 V and 0.16 V, respectively. Also, a decrease in the band gap leads to a slight increase in the short-circuit current density from 27.6 mA / cm^2 to 30.41 mA/cm^2. Despite the small dose of Cd, Na, O impurities, their presence leads to a decrease in the PCE of solar cells. PCE decreases from ~ 5 % to 2.34 %.

Table 1. The Main Output Energy Parameters

	Voc, V	Jsc, mA/cm^2	FF, %	PCE, %
CZTS	0.297	27.595	60.58	4.97
CZTS:Cd	0.187	30.282	46.07	2.61
CZTS:Na	0.277	25.674	56.37	3.3
CZTS:O	0.157	30.409	49.22	2.34

One of the main characteristics of solar cells is the JV characteristic (Fig. 5). The JV characteristic reflects the internal dynamics of a solar cell and shows the parameters that determine its output power. As can be seen, a solar cell based on an absorber contaminated with Cd, Na, O has relatively worse JV characteristics and is significantly inferior in output power from a solar cell based on a pure absorber.

The quantum yield of a solar cell based on a pure and impurity absorber is shown in Fig. 6. The quantum yield of solar cells with CZTS: Cd and CZTS: O is noticeably inferior to that of a pure absorber in the high-energy region (~ 2.8–4 eV), and in the case of CZTS: Na, on the contrary, in the low-energy region (~ 1.5–2.5 eV). We believe that this is due to a change in the band gap towards a decrease in CZTS: Cd (E_g ~ 0.9 eV) and CZTS: O (E_g ~ 0.79 eV) and an increase in the case of CZTS: Na (E_g~1.2 eV), as well as a change in their optical characteristics.

In the end, it should be noted that the important role in the functioning of various devices, including solar cells, depends on the state of their surface, defects on the surface and in the near-surface layer, surface porosity, stability of adsorbed molecules, etc. [32]–[45]. Some of these issues are in progress and will be reported in subsequent articles.

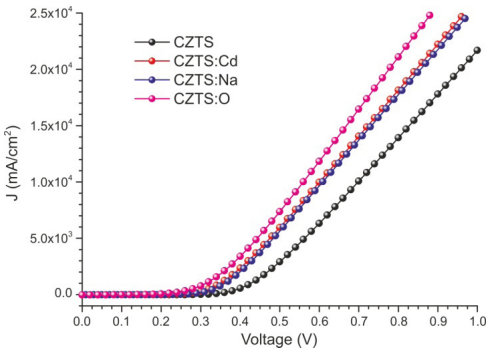

Fig. 5. JV characteristics of a solar cell based on CZTS.

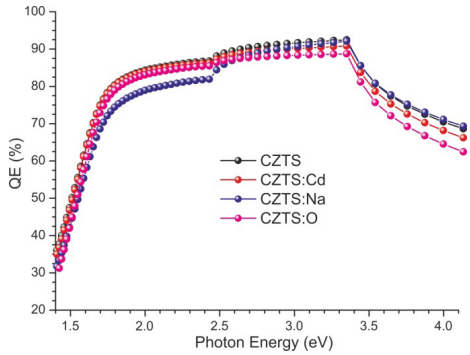

Fig. 6. CZTS based solar cell quantum yield.

4. CONCLUSIONS

Thus, in this paper, within the framework of the DFT-GGA, the optical properties of the CZTS multicomponent semiconductor absorber with a 3 % impurity of Cd, Na, O were determined, as well as their effect on the performance of CZTS solar cells was considered. It was shown that the introduction of these impurities would lead to a decrease in the intensity of the absorption spectrum at 2.06 eV and 2.55 eV. It was

revealed that impurities of Cd and O atoms would lead to a decrease in E_g CZTS to 0.9 eV and 0.79 eV, respectively, while impurities of Na atoms increased E_g to 1.2 eV. It was found that with a decrease in the band gap in CZTS: Cd, CZTS:O, the open circuit voltage V_{oc} noticeably decreased from ~ 0.3 V to 0.19 V and 0.16 V, and the indicated impurities led to a decrease in the PCE of solar cells from ~ 5 % to 2.34 %. It was shown that solar cells with impurity absorbers had poorer JV characteristics, and their quantum yield was noticeably inferior to those of a pure absorber both in the high-energy region (CZTS: Cd, CZTS: O) and in the low-energy region (CZTS: Na). The results obtained can be useful in the development of environmentally-friendly solar cells based on CZTS for future technologies.

ACKNOWLEDGEMENTS

The research has been supported by grant of the Ministry of Education and Science of the Republic of Kazakhstan AP09562784. The authors (D. Sergeyev) acknowledges the provision of SCAPS-1D software by Prof. Marc Burgelman. The research of A.I. Popov has been supported by the Institute of Solid State Physics (ISSP), University of Latvia (UL). ISSP UL as the Centre of Excellence is supported through the Framework Program for European Universities Union Horizon 2020, H2020-WIDESPREAD-01–2016–2017-TeamingPhase2 under Grant Agreement No. 739508, CAMART2 project.

REFERENCES

1. Khan, M.R., Patel, M.T., Asadpour, R., Imran, H., Butt, N.Z., & Alam, M.A. (2021). A Review of Next Generation Bifacial Solar Farms: Predictive Modeling of Energy Yield, Economics, and Reliability. *Journal of Physics D-Applied Physics*, 54 (32), 323001. DOI: 10.1088/1361-6463/abfce5
2. Veremiichuk, Y., Yarmoliuk, O., Pustovyi, A., Mahnitko, A., Zicmane, I., & Lomane, T. (2020). Features of Electricity Distribution Using Energy Storage in Solar Photovoltaic Structure. *Latvian Journal of Physics and Technical Sciences*, *5*, 18–29. DOI: 10.2478/lpts-2020-0024
3. Tao, L., Qiu, J., Sun, B., Wang, X., Ran, X., Song, L., …, & Chen, Y. (2021). Stability of Mixed-Halide Wide Bandgap Perovskite Solar Cells: Strategies and Progress. *Journal of Energy Chemistry*, *61*, 395–415. DOI: 10.1016/j.jechem.2021.03.0382095-4956
4. Bezrukovs, D., Bezrukovs, V., Bezrukovs, Vl., Konuhova, M., & Aniskevich, S. (2020). The Comparison of the Efficiency of Small Wind Turbine Generators with Horizontal and Vertical Axis under Low Wind Conditions. *Latvian Journal of Physics and Technical Sciences*, *5*, 61–72. DOI: 10.2478/lpts-2020-0028
5. Groza, E., Balodis, M., Gulbis, K., & Dirba, J. (2021). Benefits of Energy Storage Systems for Small-Scale Wind Farm Development in Latvia. *Latvian Journal of Physics and Technical Sciences*, *2*, 11–18. DOI: 10.2478/lpts-2021-0008
6. Trota, A., Ferreira, P., Gomes, L., Cabral, J., & Kallberg, P. (2019). Power Production Estimates from Geothermal Resources by Means of Small-Size Compact Climeon Heat Power Converters: Case Studies from Portugal (Sete Cidades, Azores and Longroiva Spa, Mainland). *Energies*, *12* (14), 2838. DOI: 10.3390/en12142838

7. Ciceron, J., Badel, A., & Tixador, P. (2017). Superconducting Magnetic Energy Storage and Superconducting Self-Supplied Electromagnetic Launcher. *European Physical Journal – Applied Physics*, *80* (2), 20901. DOI: 10.1051/epjap/2017160452
8. Zhang, Y., Jia, X., Liu, S., Zhang, B., Lin, K., Zhang, J., & Conibeer, G. (2021). A Review on Thermalization Mechanisms and Prospect Absorber Materials for the Hot Carrier Solar Cells. *Solar Energy Materials and Solar Cells*, *225*, 111073. DOI: 10.1016/j.solmat.2021.111073
9. Bello, M., & Shanmugan, S. (2020). Achievements in Mid and High-Temperature Selective Absorber Coatings by Physical Vapor Deposition (PVD) for Solar Thermal Application. *Journal of Alloys and Compounds*, *839*, 155510. DOI: 10.1016/j.jallcom.2020.155510
10. Kaulachs, I., Ivanova, A., Holsts, A., Roze, M., Flerov, A., Tokmakov, A., …, & Rutkis, M. (2021). Perovskite $CH_3NH_3PbI_{3-x}Cl_x$ Solar Cells. Experimental Study of Initial Degradation Kinetics and Fill Factor Spectral Dependence. *Latvian Journal of Physics and Technical Sciences*, *1*, 53–69. DOI: 10.2478/lpts-2021-0006
11. Mandal, P., Debbarma, J., & Saha, M. (2021). A Review on the Emergence of Graphene in Photovoltaics Industry. *Biointerface Research in Applied Chemistry*, *11* (6), 15009–15036. DOI: 10.33263/BRIAC116.1500915036
12. Sergeyev, D.M., & Duisenova, A.G. (2021). Electron Transport in Model Quasi-Two-Dimensional van der Waals Nanodevices. *Technical Physics Letters*, *47* (4), 375–378. DOI: 10.1134/S1063785021040295
13. Meng, Zh., Stolz, R.M., Mendecki, L., & Mirica, K.A. (2019). Electrically-Transduced Chemical Sensors Based on Two-Dimensional Nanomaterials. *Chem. Rev*, *119*, 478–598. DOI: 10.1021/acs.chemrev.8b00311
14. Koch, R.J., Konstantinova, T., Abeykoon, M., Wang, A., Petrovic, C., Zhu, Y., …, & Billinge, L. (2019). Room Temperature Local Nematicity in FeSe Superconductor. *Phys. Rev. B, 100*, 020501. DOI:10.1103/PhysRevB.100.020501
15. Sergeyev, D.M. (2013). Plasma Frequency in Josephson Junctions with a Non-Sinusoidal Current-Phase Relation. *Solid State Phenomena*, *200*, 272–275. DOI: 10.4028/www.scientific.net/SSP.200.272
16. Sergeyev, D.M. (2012). About Tunneling of Pairs of the Cooper Pairs through the Josephson Junctions in Exotic Superconductors. *Russian Physics Journal*, *55* (1), 84–91. DOI: 10.1007/s11182-012-9779-4
17. Balakhayeva, R., Akilbekov, A., Baimukhanov, Z., Usseinov, A., Giniyatova, S., Zdorovets, M., …, & Dauletbekova, A. (2021). CdTe Nanocrystal Synthesis in SiO2/Si Ion-Track Template: The Study of Electronic and Structural Properties. *Physica Status Solidi A*, *218* (1), 2000231. DOI: 10.1002/pssa.202000231
18. Sergeyev, D.M. (2018). Computer Simulation of Electrical Characteristics of a Graphene Cluster with Stone-Wales Defects. *J. Nano-Electron. Phys., 10* (3), 03018. DOI: 10.21272/jnep.10(3).03018
19. Chuan, M.W., Lau, J.Y., Wong, K.L., Hamzah, A., Alias, N.E., Lim, C.S., & Tan, M.L.P. (2021). Low-Dimensional Modelling of n-Type Doped Silicene and its Carrier Transport Properties for Nanoelectronic Applications. *Advances in Nano Reseach*, *10* (5), 415–422. DOI: 10.12989/anr.2021.10.5.415
20. Sergeyev, D. (2021). One-Dimensional Schottky Nanodiode Based on Telescoping Polyprismanes. *Advances in Nano Reseach*, *10* (4), 339–347. DOI: 10.12989/anr.2021.10.4.339
21. Zeng, X., Lontchi, J., Zhukova, M., Fourdrinier, L., Qadir, I., Ren, Y., …, & Flandre, D. (2021). High-Responsivity Broadband Photodetection of an Ultra-Thin In_2S_3/CIGS Heterojunction on Steel. *Optics Letters*, *46* (10), 2288–2291. DOI: 10.1364/OL.423999
22. Witte, W., Hempel, W., Paetel, S., Menner, R., & Hariskos, D. (2021). Effects of Sputtered In_xS_y Buffer on CIGS with RbF Post-Deposition Treatment. *ECS Journal of Solid State Science and Technology*, *10* (5), 055006. DOI: 10.1149/2162-8777/abfc21

23. Yang, H., Jiang, G., Wang, W., & Mei, X. (2021). Femtosecond Laser Fabrication of Micro and Nano-Structures on CIGS/ITO Bilayer Films for Thin-Film Solar Cells. *Materials*, *14* (9), 2413. DOI: 10.3390/ma14092413

24. Novikov, G.F., & Gapanovich, M.V. (2017). Third Generation Cu-In-Ga-(S,-Se) Based Solar Inverters. *Phys. Usp*., *60*, 161–178. DOI: 10.3367/UFNe.2016.06.037827

25. Milichko, V.A., Shalin, A.S., Mukhin, I.S., Kovrov, A.E., Krasilin, A.A., Vinogradov, A.V., …, & Simovskii, C.R. (2016). Solar Photovoltaics: Current State and Trends. *Phys. Usp*., *59*, 727–772.DOI: 10.3367/UFNe.2016.02.037703

26. Smidstrup, S., Stradi, D., Wellendorff, J., Khomyakov, P.A., Vej-Hansen, U.G., Lee, M-E., …, & Stokbro, K. (2017). First-Principles Green's-Function Method for Surface Calculations: A Pseudopotential Localized Basis Set Approach, *Phys. Rev. B*, *96*, 195309. DOI: 10.1103/PhysRevB.96.195309

27. *Atomistix ToolKit*. Manual Version. (2015). *QuantumWise A/S,* 1, 840.

28. Burgelman, M., Nollet, P., & Degrave, S. (2000). Modelling Polycrystalline Semiconductor Solar Cells. *Thin Solid Films*, *361–362*, 527–532. DOI: 10.1016/S0040-6090(99)00825-1

29. Decock, K., Zabierowski, P., & Burgelman, M. (2012). Modeling Metastabilities in Chalcopyrite-Based Thin Film Solar Cells. *Journal of Applied Physics*, *111*, 043703. DOI: 10.1063/1.3686651

30. Burgelman, M., Decock, K., Khelifi, S., & Abass, A. (2013). Advanced Electrical Simulation of Thin Film Solar Cells. *Thin Solid Films*, *535*, 296–301. DOI: 10.1016/j.tsf.2012.10.032

31. Decock, K., Khelifi, S., & Burgelman, M. (2011). Modelling Multivalent Defects in Thin Film Solar Cells. *Thin Solid Films*, *519*, 7481–7484. DOI: 10.1016/j.tsf.2010.12.039

32. Sychikova, Y.A., Kidalov, V.V., & Sukach, G.A. (2013). Dependence of the Threshold Voltage in Indium-Phosphide Pore Formation on the Electrolyte Composition. *J. Synch. Investig., 7,* 626–630. DOI: 10.1134/S1027451013030130

33. Suchikova, J. A. (2015). Synthesis of Indium Nitride Epitaxial Layers on a Substrate of Porous Indium Phosphide. *Journal of Nano- and Electronic Physics*, *7* (3), 3017–1.

34. Eglitis, R., Purans, J., Popov, A. I., & Jia, R. (2019). Systematic Trends in $YAlO_3$, $SrTiO_3$, $BaTiO_3$, $BaZrO_3$ (001) and (111) Surface *ab initio* Calculations. *International Journal of Modern Physics B*, *33* (32), 1950390. DOI: 10.1142/S0217979219503909

35. Eglitis, R., Popov, A. I., Purans, J., & Jia, R. (2020). First Principles Hybrid Hartree-Fock-DFT Calculations of Bulk and (001) Surface F Centers in Oxide Perovskites and Alkaline-Earth Fluorides. *Low Temperature Physics*, *46* (12), 1206–1212. DOI: 10.1063/10.0002475

36. Eglitis, R. I., Purans, J., Gabrusenoks, J., Popov, A. I., & Jia, R. (2020). Comparative *ab initio* Calculations of ReO_3, $SrZrO_3$, $BaZrO_3$, $PbZrO_3$ and $CaZrO_3$ (001) Surfaces. *Crystals*, *10* (9), 745. DOI: 10.3390/cryst10090745

37. Rusevich, L. L., Kotomin, E. A., Zvejnieks, G., & Popov, A. I. (2020). *Ab initio* Calculations of Structural, Electronic and Vibrational Properties of $BaTiO_3$ and $SrTiO_3$ Perovskite Crystals with Oxygen Vacancies. *Low Temperature Physics*, *46* (12), 1185–1195. DOI: 10.1063/10.0002472

38. Krainyukova, N. V., Hamalii, V. O., Peschanskii, A. V., Popov, A. I., & Kotomin, E. A. (2020). Low Temperature Structural Transformations on the (001) Surface of SrTiO3 Single Crystals. *Low Temperature Physics*, *46* (7), 740–750. DOI: 10.1063/10.0001372

39. Krainyukova, N. V., Kuchta, B., Firlej, L., & Pfeifer, P. (2020). Absorption of Atomic and Molecular Species in Carbon Cellular Structures. *Low Temperature Physics*, *46* (3), 219–231. DOI: 10.1063/10.0000705

40. Suchikova, Y., Vambol, S., Vambol, V., & Mozaffari, N. (2019). Justification of the Most Rational Method for the Nanostructures Synthesis on the Semiconductors Surface. *Journal of Achievements in Materials and Manufacturing Engineering*, *92* (1–2), 19–28.

41. Ananyev, M. V., Porotnikova, N. M., & Kurumchin, E. K. (2019). Influence of Strontium Content on the Oxygen Surface Exchange Kinetics and Oxygen Diffusion in $La_{1-x}Sr_xCoO_{3-\delta}$ Oxides. *Solid State Ionics*, *341*, 115052. DOI: 10.1016/j.ssi.2019.115052

42. Osinkin, D.A., Khodimchuk, A.V., Porotnikova, N.M., Bogdanovich, N.M., Fetisov, A.V., & Ananyev, M.V. (2020). Rate-Determining Steps of Oxygen Surface Exchange Kinetics on $Sr_2Fe_{1.5}Mo_{0.5}O_{6-\delta}$. *Energies*, *13*, 250. DOI: 10.3390/en13010250

43. Porotnikova, N. M., Vlasov, M. I., Zhukov, Y., Kirschfeld, C., Khodimchuk, A. V., Kurumchin, E. K., ..., & Ananyev, M. V. (2021). Correlation between Structure, Surface Defect Chemistry and $^{18}O/^{16}O$ Exchange for $La_2Mo_2O_9$ and $La_2(MoO_4)_3$. *Physical Chemistry Chemical Physics*, *23* (22), 12739–12748. DOI: 10.1039/D1CP00401H

44. Hamalii, V. O., Peschanskii, A. V., Popov, A. I., & Krainyukova, N. V. (2020). Intrinsic Nanostructures on the (001) Surface of Strontium Titanate at Low Temperatures. *Low Temperature Physics*, *46* (12), 1170–1177. DOI: 10.1063/10.0002470

45. Ostanina, T. N., Rudoi, V. M., Nikitin, V. S., Darintseva, A. B., Zalesova, O. L., & Porotnikova, N. M. (2016). Determination of the Surface of Dendritic Electrolytic Zinc Powders and Evaluation of its Fractal Dimension. *Russian Journal of Non-Ferrous Metals*, *57* (1), 47–51. DOI: 10.3103/S1067821216010120